

IMPROVING LASER COHERENCE

JOHN L HALL^{*}, MARK NOTCUTT, AND JUN YE[†]

*JILA, University of Colorado and
National Institute of Standards and Technology
Boulder, CO 80309-0440 USA*

The convenient approximation of a real laser field by a Coherent State is again a relevant topic of interest, as laser spectroscopy scenarios are being developed in which remarkably long atomic lifetimes and extended interaction times (~ 100 s) can be enjoyed. Years ago, appropriate locking techniques were shown to allow precise locking of a laser field to a cavity, even in the milliHz domain, but lab vibrations modulated the cavity length and so the obtained optical frequency. Methods such as mechanical isolation (on a heroic scale) or active anti-vibration approaches are sufficiently productive such that, by now several groups have developed visible optical sources with \sim Hz linewidths. Still, linewidths in the 100 milliHz domain have seemed very challenging — all the margins have been used up. We discuss mounting systems for an optical reference cavity, particularly an improved one based on implementing vertical symmetry, which provides dramatic reduction in the vibration sensitivity and can yield sub-Hz linewidths on an ordinary optical table in an ordinary lab. Interesting and commanding new issues — such as temporally-dependent spatial structure of the EO-modulated probe beam, and thermally-generated mechanical position noise — are found to dominate the laser phase errors in the sub-Hz linewidth domain. The theoretical scaling — and the spectral character — of this thermal noise motion of the cavity mirror surfaces have been studied and confirmed experimentally, showing an $\sim 1 \times 10^{-16}$ m/Sqrt(Hz) thermal noise amplitude at 1 Hz, with a $1/\text{Sqrt}(f)$ amplitude spectral density, with f being the Fourier frequency of this noise process. For effective temperature stabilization, multi-point thermal control and dual thermal shells provide stable operation near the ULE thermally-stationary point. Spectral filtering in the optical and vacuum paths is critically important to prevent ambient thermal radiation from entering the inner shell. The observed frequency drift-rate of ~ 0.05 Hz/s is not yet ideally stable, but it appears possible to compensate drift accurately enough to allow 1 radian coherence times to approach ~ 100 s — *if* other problems such as the thermal noise can be adequately suppressed. Recent JILA spectra of lattice-trapped cold Sr atoms show an excellent prospect for ultrahigh resolution spectroscopy and highly stable optical atomic clocks and make us anxious to perfect improved phase-stable laser sources for the $^1S_0 - ^3P_0$ doubly-forbidden transition at 698 nm. These laser developments are aided by optical comb techniques, allowing useful phase comparison of several prototype stable laser sources, despite their various different wavelengths.

^{*} Formerly also with Quantum Physics Division, National Institute of Standards and Technology.

[†] Also with Quantum Physics Division, National Institute of Standards and Technology.

1.1. *Optical Frequency Coherence - In the Beginning*

Initially, laser coherence was quantified in “Gillette” units. It was not the razor blade’s sharp edges that could help define a position, but rather their darkened color and convenient thinness such that a diffraction-limited Ruby laser of about $\frac{1}{4}$ Joule was already able to punch a hole through a blade’s thickness. Spatially less-coherent lasers would require about 1 Joule/Gillette. Regrettably, every Q-switched laser pulse was different: “Doing science” with early laser tools was indeed exciting! Nonlinear physics was clearly visible, but hard to study in a fully controlled way. A JILA study of optically-induced level shifts in potassium vapor showed rates scaling like Angstroms per MW/cm², but with frustrating irreproducibility due to uncontrolled spectral and geometrical structure of the ruby laser’s output. We chose to go fishing in calmer waters, where kHz shifts per milliWatt/cm² would be the scale. It would be — and still is — done with cw lasers and can be highly quantitative. And now frequency comb technology makes it almost easy!

The early cw gas lasers had relatively narrow emission linewidths, since their gain media were stable and their low gain required use of low loss cavities. The milliWatt output power with such a cavity gave Schawlow-Townes phase-diffusion linewidths calculated to be in the milliHz domain. Of course it was quickly understood that vibrations were influencing the length of the laser cavity in a profound way, so the precision level was more like kHz or even MHz, rather than the expected milliHz. So early in the laser’s history anti-vibration activities began in earnest, using remote facilities such as the old wine cellar at MIT and inactive gold mines, such as the Poorman’s Relief Gold Mine, in the mountains about 20 minutes west of Boulder [1].

But the approach of “hiding away” was destined to be limiting: By the mid 1970’s interesting new tunable dye lasers could achieve almost any wavelength, but the electric power and cooling water required for their Argon-ion pump lasers would be enough to support the good life in a whole neighborhood. Already in 1973, the first year of cw dye lasers, opto-electronic servo-control methods were used to make even a dye laser achieve a narrow linewidth [2]. The concept was to use a reference Fabry-Perot cavity of adequate finesse, such that the shot-noise limit in finding its resonance center could be adequately small. We were thrilled to achieve fast linewidths in the order of 1 kHz, unfortunately contaminated by vibration-induced frequency noise perhaps one or two orders larger. A wonderful collaboration between spectroscopists and Gravitational Wave Detector communities led to the now-standard scheme [3] of using RF modulation sidebands as the phase reference for measuring the

phase-shift of the leakage field emerging again from the input mirror of the reference cavity. This RF-based discriminator, sometimes referred to as the Pound-Drever-Hall technique, has many wonderful properties as an optical phase/frequency discriminator, as did its conceptual predecessor that had been used by Robert Pound more than a quarter-century earlier for cavity stabilization of microwave oscillators in Radar systems. Locking to optical cavity modes at the Hz level was soon demonstrated [4] .

1.2. *Stable Lasers are Needed!*

But the attained laser frequency stability soon grew to be inadequate as ion trapping and cold atom magneto-optics traps (MOT's) became widespread. As a community, we arrived at the funny place that we could manage vacuums in the 10^{-10} torr range, trap ions for hours, cool them to nearly the ground state of vibration in their trapping potential — serious high-tech achievements. But almost no group had the sub-100 Hz laser needed to probe such delicious spectroscopic samples. Of course, major labs could and did attack the laser vibrational incoherence problem with great energy — and money — by building elaborate and expensive vibration isolated rooms. Pioneering work in this regard was done by Jim Bergquist and his colleagues in NIST Boulder, and their published 0.22 Hz linewidth [5] of a laser beatnote remains the world record.

Another anti-vibration approach would be active anti-seismic servo systems: eventually our JILA labs were able to record 60 dB reductions of the vertical accelerations of an optical table around 1 Hz. But mode coupling is an important issue when the MultiInput-MultiOutput (MIMO) control system has been carefully tuned for orthogonalization of the responses. A screwdriver for Allen cap screws, carelessly left on the table, could cost a factor 2 in the noise level at the cavity, due to changed coupling with a less-well-cooled tilt mode.

A better active anti-vibration campaign has been pursued by MPQ [6] and by NPL [7], using recently-available 6 Degrees-of-Freedom active vibration-reducing modules [8], which offer more than 20 dB improvement over the band 3–100 Hz. Starting from a quiet environment, or if “stacking” such attenuators, the ultimate limit is set by the acceleration sensing noise, $\sim 100 \text{ ng}/\sqrt{\text{Hz}}$.

As an alternative, passive isolating platforms are available [9] with $\sim 1/2$ Hz resonance and >30 dB isolation above 3 Hz. The $Q \sim 5$ resonance leads to a $1/e$ decay time < 1 s, so even a 1 mm-scale disturbance decays to near the background level in only ~ 10 s . With either passive or active isolation, the long-term tilt stability of the platform may be challenging for many cavity designs, because of tilt-induced distortions associated with gravity.

As for design, early on it seemed “obvious” that axial accelerations of the optical cavity would be the painful ones, and an effective single-degree of isolation suspension system for the cavity spacer was created by using 5 wires [10]. This idea was indeed somewhat effective, but at the time the cavity stiffness was compromised by inclusion of a PZT transducer. That led to many generations of optically-contacted reference cavities at JILA, and elsewhere. Figure 1 shows measured vertical acceleration sensitivity of two possible mountings of such a cavity. The mounting originally used the spacing $B = 0.11 L$. This short distance of $B/L = 0.11$ between the mounting points was chosen to reduce coupling of temperature-induced length changes of the support system into cavity changes. The special “Airy” separation of $B = 0.577 L$ was used for metrology work with end gauges, as their end faces are then parallel [11]. This change made a most welcome 15-fold reduction of vertical vibrations being converted into frequency fluctuations. We still do not have a good explanation for the large sensitivity of the *shorter*-spacing case. The easy explanation in terms of a longitudinal Doppler shift seems unlikely since there is no strong image of the rocking modes, or the 2 Hz axial swinging resonance. Rather, it is believed that transverse forces from non-vertical mounting straps were incompletely isolated by the first mounting system: This reality is shown by a step temperature change of the inner shell having an impact on frequency within

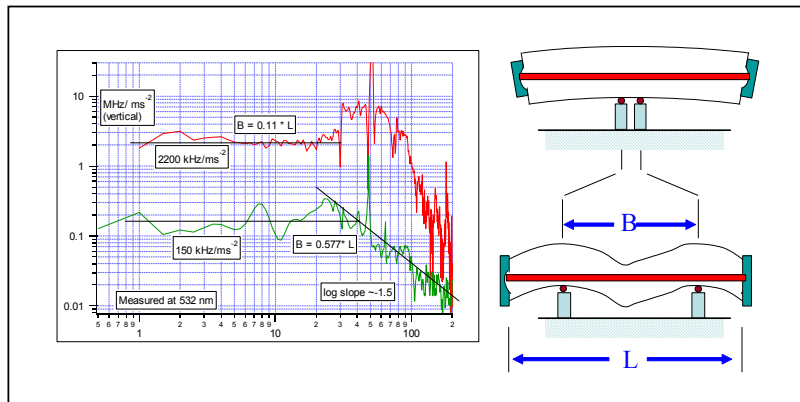


Fig.1. Measured vertical acceleration frequency sensitivity of ULE bar, 27.7 cm L , x 7.1 cm wide x 5.7 cm tall. A mechanical low-pass filter was added to reduce vibrations above ~ 30 Hz in the Airy mounting case (lower part of Fig. 1.)

the ~minute time scale it may take for diffusion to bring the new temperature to the inner surface. The thermal radiative coupling ultimately can also be seen, appearing as a weak frequency ramp, due to the thermal integration.

With uniform support under a horizontal cavity's whole length, we expect

$$\boxed{\frac{\delta f}{f} = -\frac{\delta L}{L} = \frac{\rho \sigma h}{2Y} a} \quad (1)$$

where ρ is the ULE density (2.21 gm/cm³), σ is the Poisson ratio (~0.17), Y is the Young's modulus (67 GPa), h is the bar's height, and a is the acceleration. This frequency/acceleration sensitivity evaluates to 90 kHz/ms⁻² predicted, vs. ~150 kHz/ms⁻² observed with the Airy support. (Actually, the wider face of this ULE cavity rests in four places, provided by two heavy-wall O-rings at the Airy separation on each of two longitudinal supporting Zerodur rods of 25.4 mm diameter, 50 mm center/center spacing.) Again, transverse forces may play a role. For comparison, the measured response was 180 kHz/ms⁻² for a 250 mm long cavity supported via Vee-blocks near the bottom of its 100 mm diameter .

1.3. *Vibrational Noise Input, Analysis of its Consequences*

We now consider the vibrational input part of the frequency noise question. A widely used model for seismic noise in quiet lab locations, confirmed in our QuietRoom Lab at JILA, is a vertical noise density of about 1×10^{-8} m/Sqrt(Hz) from 1 Hz to 30 Hz, falling above 30 Hz as f^{-2} , and rising below 1 Hz roughly as f^{-3} . (The highly variable microseism peak at ~0.16 Hz can be enhanced strongly by storms near the continental coastline.) A noise that is spectrally flat in a position description will have a rising density ($\sim f^2$) plotted as acceleration. An air-floating table introduces ideally a $\sim 1/f^2$ filter function, leading to a table-top acceleration noise roughly flat with frequency up to ~100 Hz. Figure 2a shows our vertical acceleration data and in 2b the calculated frequency variation spectral density, based on the properties of the rectangular ULE bar-cavity in the Airy-style suspension noted before.

Given some FM frequency deviation density $Sqrt(S_v(f))$ in Hz/Sqrt(Hz), as induced by vibrations at frequency f , there is a corresponding Phase Modulation density $Sqrt(S_\phi(f)) = Sqrt(S_v(f))/f$. For sinewave modulation we would speak of the phase modulation index $\beta = \text{peak frequency deviation } \delta f / \text{deviation rate } f$. FM theory describes the generation of pairs of new optical frequencies, offset from the laser by multiples of the modulation frequency f . For a small modulation index, one produces only the first pair (upper and lower sideband) of lines straddling the laser central frequency, and each line will carry a relative power of $J_1(\beta)^2 \equiv (\beta/2)^2$. With noise processes, integrating over a little bandwidth

around f also leads to a phase modulation index, and transfers some laser power out of the bright line carrier. The modulations at high frequencies are inefficient, due to the factor f in the denominator of the ratio defining β . If we look with low spectral resolution at the optical frequency, none of the modulations will be revealed: we will see the full laser power, integrated over its spectrum.

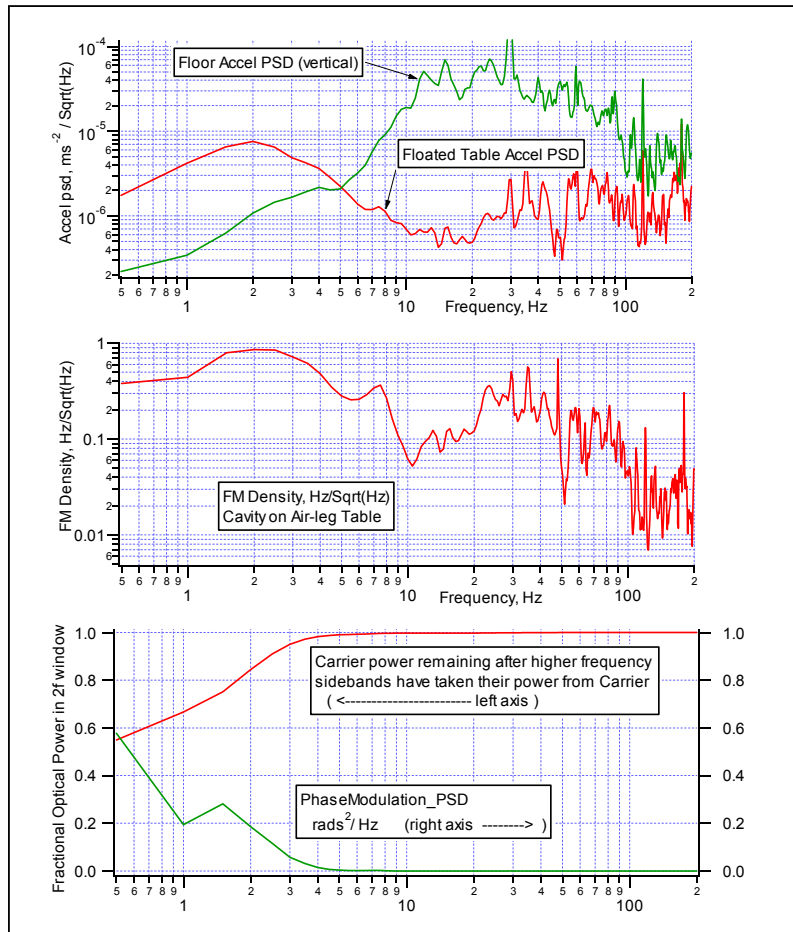


Fig. 2. Evaluation of remaining carrier, vs. frequency. Small broadband vertical vibration gives rise to a related FM spectrum, by distorting the reference cavity. See text for discussion of sideband generation and reduction of the optical carrier power. Eventually, coherence of any small remaining “carrier” component is limited by other noise sources in the locking process. Evaluated for 532 nm.

However with increasing resolution, we begin to isolate the sideband power as shifted to high frequencies by fast modulation processes. The laser power remaining in the resolution bandwidth, being only carrier and close-in sidebands, is less than the previous total power. Continuing this process we will eventually come to find the resolving bandwidth that leaves just half of the total power in the acceptance window. This operationally defines the laser's FWHM optical power bandwidth. For the calculation of carrier loss, we start at high frequencies and integrate the phase-squared spectral contributions to find the rms phase deviations $\theta^2(f)$ due to fluctuations at frequencies higher than our reference frequency f . Walls and deMarchi [12] showed that the power remaining inside the band of width $2f$ centered on the optical carrier is given by $\exp(-\theta^2(f))$. This calculated remaining carrier is given as a function of frequency in Fig. 2c. Because of the exponential sensitivity, it can be seen that this cavity-based system could ideally (and just barely) generate a laser power linewidth at the 1 Hz level. Any mechanical resonances are unwelcome, as one easily can use up $\frac{1}{2}$ of the total power for their sidebands. The atoms in the MOT may still respond to this field's remaining coherent central spike, but such a laser could not be said to have a narrow FWHM bandwidth. From the vibration standpoint, we are just on the edge of having a 1-Hz laser linewidth with this horizontally-mounted system. Due to other noise sources in the locking system, discussed below, the bright-line "carrier" of our model does not have a vastly longer coherence time.

1.4. A Vertically-Mounted Cavity Design

With such experiences, seeking a fresh outlook, our group decided to attempt to reduce acceleration sensitivity *by design*. The useful role of vertical mounting to allow use of symmetry had been noted earlier by Notcutt and Blair [13], and by Hall [14]. Mounting from the midplane of the vertical cylindrical cavity would lead to equal — but opposite — length changes of both bottom and top halves, and thus a net cavity end-to-end length change near to zero. So what reduction factor should one expect? The required mechanical precision can be estimated from the expression for axial compression, holding the cavity vertically — without symmetry — from one end alone:

$$\boxed{\frac{\delta l}{l} = -\frac{\delta L}{L} = \frac{\rho L}{2Y} a} \quad (2)$$

Compared with Eq. (1), this predicted sensitivity is larger by a serious factor, $L/(\sigma^*h)$, a factor of $\sim 5x$ from dimensions and $\sim 5x$ again from loss of the Poisson ratio. This scale is 28-fold larger (V vs H) for the cavity of Fig. 1.

However, using the symmetry idea, in the machining of the structure we can expect a precision of, say, 0.1 mm out of, say, 100 mm cavity length. This is an asymmetry factor of $\epsilon = 2/1000$ in our favor. So a nominally-fabricated vertical cavity should be able to give us a sensitivity $\sim 20\times$ reduced from that calculated for horizontal use. While the shortening to 100 mm cavity length seems prudent considering its weight, it also reduces the sensitivity. Again, Finite-Element modeling reveals complexity associated with details of the support. Projecting monolithic “ears,” and different contacting ideas (point-like vs. finite area) were considered. From Fig. 3 several facts are clear: The basic distortions are substantially larger, but are nearly matched so that the net sensitivity is both small and can be trimmed toward zero by adding small weights

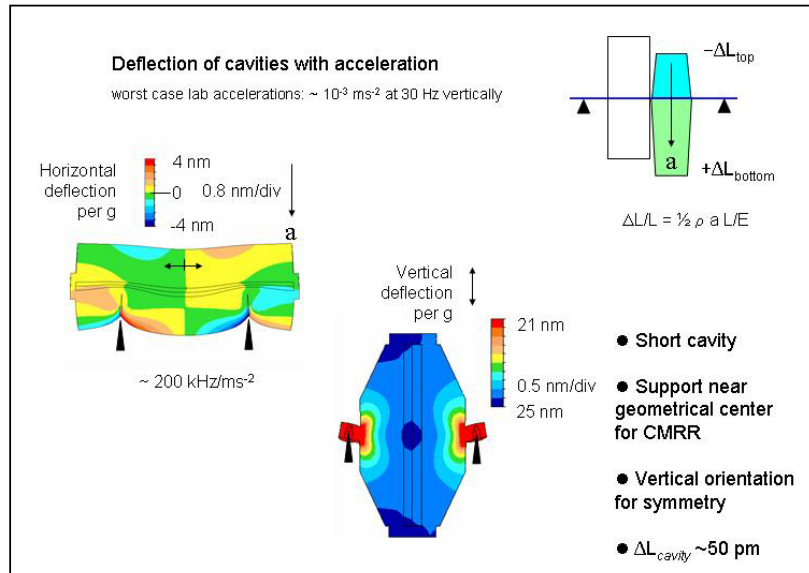


Fig. 3. Calculated distortions under 1 g vertical acceleration. While the axial distortion is of a smaller scale with horizontal mounting, there is no case where the distortion is zero. The vertical cavity requires fabrication care, but gives a plane of null sensitivity, and a convenient “tweaking” avenue.

The experimental trial used an available ULE cavity of 50 mm length and 12.5 mm diameter, having a finesse $\sim 46 \times 10^3$ and a linewidth of 65 kHz. This length approximates the height of our first cavity, but we lose the favorable $\sigma = 0.17$ factor in Eq. (1). Support at the vertical midplane was approximated by mounting the cavity into a Zerodur disk, drilled to accept the cavity’s diameter,

plus a $\frac{1}{4}$ mm gap to be filled with silicone RTV adhesive. The length-wise centering was accurate to ~ 0.5 mm. The disk had been pre-drilled to its mid-plane from both faces to provide two sets of 3 holes which could receive the 3 vertical mounting posts. (See Fig. 4.) With the lighter end up, one could add bits of In (indium) wire on the top to increase the acceleration sensitivity of this less-sensitive half. In this way the coefficient (observed at 1064 nm) could be trimmed from ~ 18 to below 10 kHz/ms^{-2} [15], limited by cross-coupling and inequivalence of the PZT shakers under each of the 3 legs. For comparison, Eqs. 1 and 2 predict 9.8 kHz/ms^{-2} for horizontal and 232 kHz/ms^{-2} for unsymmetrical vertical mounting (at 1064 nm). So by “going vertical” we lost the $\sigma = 0.17$ factor and accepted a longer scale length, but even our imperfect mounting symmetry bought us a factor $\sim 23x$ reduction of the nominal vertical acceleration sensitivity. By use of more precise fabrication symmetry, we can win a net sensitivity reduction factor at a particular length, plus we have the ability to trim to even better reduction. Also the smaller cavity and vertical geometry is better for using dual-layer thermal controls: readily-available ULE needs cooling to reach its zero CTE point and the Peltier coolers need a big surface for their heatsink. The vertical geometry can also be used with a spherical or doubled-cone overall cavity shape that can provide a calculated acceleration sensitivity reduction of about $3x$ relative to the full cylindrical spacer.

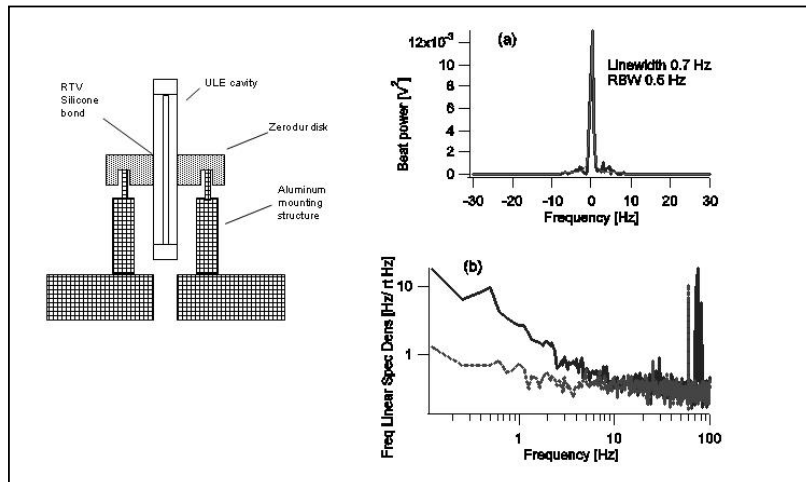


Fig. 4. Performance of Vertically-Mounted Cavity. The acceleration sensitivity is reduced about 25-fold by the attained symmetry, compared to the case of vertical cavity held from one end. Part a) shows sub-Hz beat linewidth between two vertical systems. In b), frequency noise density of beat rises at low frequency above discriminator noise, consistent with mirror thermal noise. See below.

1.5. Unwelcome News from Thermodynamics: Thermal Mechanical Noise

For several years the Gravitational Wave community has been interested in the sub-femtometer mechanical motions that result from back-coupling of thermal energy into mechanical motions [16]. The process can be understood via the Fluctuation-Dissipation Theorem as a kind of time-reversed ultrasonic absorption process, where the coupling constant is basically the ultrasonic loss, expressible in terms of inverse mechanical Q-factor. Interestingly, popular choices of suitable optical materials — fused silica, ULE, Zerodur and Tantalum-based HR coatings [17, 18] — vary by a factor 30 in their mechanical losses. Numata *et al.* [19] present a useful noise model, and quote assumed losses, $1/Q$, for ULE, fused silica, Zerodur, and HR coatings of $(1/6 \times 10^4)$, $(1/1 \times 10^6)$, $(1/3 \times 10^3)$, and $(1/4 \times 10^4)$, respectively. The frequency density measurements of Fig. 5 approximate the expected $1/f^{1/2}$ noise rise at low frequencies. Our numerical values are estimated from the lowest parts of our curves, and are typically about 2-fold larger than predicted by the Numata model. It is likely that optical contact noise is contributing also. The summary of these findings is that, to achieve laser coherence times of even ~ 10 s, it will be necessary to pay careful attention

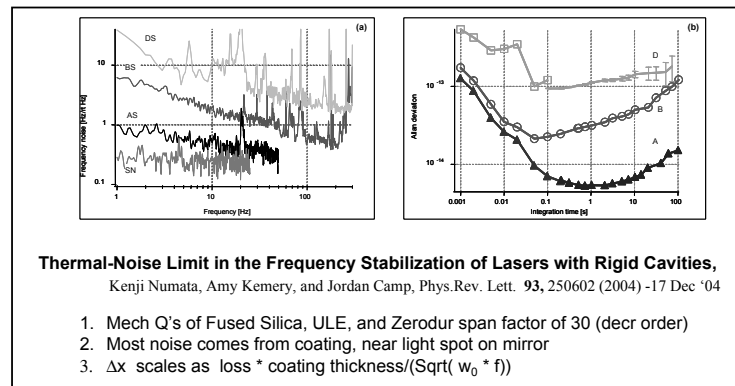


Fig 5. Low frequency increase of frequency noise, due to thermal-mechanical noise of the mirrors' surfaces. Amplitude scale is $\sim 3 \times 10^{-16}$ m/Sqrt(Hz) at 1 Hz, with $1/\text{Sqrt}(f)$ predicted dependence. The lowest noise, case A, is for the ULE standard of Fig. 4 beating with a 3.5 cm cavity fitted with fused silica mirrors. In case B those mirrors are replaced with Zerodur substrate ones with similar finesse. Case D uses these Zerodur mirrors on a 10 mm Zerodur spacer. The associated spectra in Fig. 5A show the rising noise at low frequencies as expected from thermal noise causes (similar in magnitude, but somewhat larger in slope). Some added noises (perhaps associated with the optical contacts, or with drift instabilities) makes the comparison of spectral slopes less clear.

to mechanical Q's and losses, and perhaps to use reference cavity lengths rather longer than ideal for vibration isolation purposes. Of course, at much longer measuring times the cavity approach to laser stabilization will show more frequency uncertainty as compared with an ensemble of cold atoms. The absolute, and the merely stable, frequency reference systems complement each other well. The next few years should see some more interesting advances!

Acknowledgments

As always, we thank Professor Long-Sheng Ma for his strong contributions, here to the vertical cavity effort. Lisheng Chen developed useful insights for us from his Finite Element modeling work. We thank Andrew Ludlow and Seth Forman for collaboration on comparing cavity stabilization of his 698 nm diode-laser system with our 1064 nm Nd systems. This work has been funded in part by the National Institute of Standards and Technology, NASA, the National Science Foundation, and by the Office of Naval Research under its MURI with the University of Colorado.

References

1. J. Levine and J. L. Hall, *Journ. Geophys. Res.*, **77**, 2595 (1972).
2. R. L. Barger, M. S. Sorem, *et al.*, *Appl. Phys. Lett.*, **22**, 573 (1973).
3. R. W. P. Drever, J. L. Hall, *et al.*, *Appl. Phys. B*, **B31**, 97 (1983).
4. C. Salomon, D. Hils, *et al.*, *J. Opt. Soc. Am. B*, **5**, 1576 (1988).
5. B. C. Young, R. J. Rafac, *et al.*, in *Laser Spectroscopy 1999*, ed. by R. Blatt, J. Eshner, *et al.* (World Scientific, Singapore, 1999) p61.
6. A. Y. Nevsky, M. Eichenseer, *et al.*, *Opt. Comm.*, **210**, 91 (2002).
7. S. A. Webster, Oxborrow, M., and Gill, Patrick, *Opt. Lett.*, **29**, 1497 (2004).
8. www.Halcyonics.de .
9. www.MinusK.com .
10. J. Hough, D. Hils, *et al.*, *Appl. Phys. B*, **33**, 179 (1984).
11. W. R. Moore, *Foundations of Mechanical Accuracy*, Moore Tool Company, Bridgeport, CT 06607, (1970).
12. F. L. Walls and A. Demarchi, *IEEE Trans. Instrum. Meas.*, **24**, 210 (1975).
13. M. Notcutt, C. T. Taylor, *et al.*, *Cryogenics*, **36**, 13 (1996).
14. J. L. Hall, *Proceedings of the SPIE*, **1837**, 2 (1993).
15. M. Notcutt, L. S. Ma, *et al.*, *Opt. Lett.*, **30**, 1815 (2005).
16. Y. Levin, *Phys. Rev. D*, **57**, 659 (1998).
17. D. R. M. Crooks, G. Cagnoli, *et al.*, *Class. Quantum Grav.*, **21**, S1059–S1065 PII: S0264 (2004).
18. Trade names are used only for purposes of technical communication.
19. K. Numata, A. Kemery, *et al.*, *Phys. Rev. Lett.*, **93**, 250602 (2004).